IVUS-based Histology of Atherosclerotic plaques: Improving Longitudinal Resolution

Arash Taki[a], Olivier Pauly [b], S.Kamaledin Setarehdan [c], Gozde Unal [a]and Nassir Navab [a]

[a]Department of Computer Aided Medical Procedures (CAMP), Technical University of Munich(TUM), Munich, Germany

[b]Control and Intelligent Processing Center of Excellence,School of Electrical and Computer Engineering, College of Engineering, University of Tehran,Tehran, Iran

[c]Faculty of Engineering and Natural Sciences, Sabanci University, Turkey

ABSTRACT

Although Virtual Histology (VH) is the in-vivo gold standard for atherosclerosis plaque characterization in IVUS images, it suffers from a poor longitudinal resolution due to ECG-gating. In this paper, we propose an image-based approach to overcome this limitation. Since each tissue have different echogenic characteristics, they show in IVUS images different local frequency components. By using Redundant Wavelet Packet Transform (RWPT), IVUS images are decomposed in multiple sub-band images. To encode the textural statistics of each resulting image, run-length features are extracted from the neighborhood centered on each pixel. To provide the best discrimination power according to these features, relevant sub-bands are selected by using Local Discriminant Bases (LDB) algorithm in combination with Fisher's criterion. A structure of weighted multi-class SVM permits the classification of the extracted feature vectors into three tissue classes, namely fibro-fatty, necrotic core and dense calcified tissues. Results shows the superiority of our approach with an overall accuracy of 72% in comparison to methods based on Local Binary Pattern and Co-occurrence, which respectively give accuracy rates of 70% and 71%.

1. INTRODUCTION

In western countries, atherosclerosis is the major cause of sudden death or disability. Sudden death is mostly related to the rupture of atherosclerotic lesions or, in other words, vulnerable plaque in the coronary artery.[1] Such lesions show four main tissue components, namely Dense Calcium (DC), fibrous, Necrotic Core (NC), and lipid rich tissues. Their size and pattern defines the staging of the disease.[2] Thus, the identification and precise tissue characterization of atherosclerosis would provide: (a) a better understanding of the disease; (b) an enhanced diagnosis to choose the appropriate treatment strategy; (c) an assessment of the therapy effectiveness.

Grayscale intravascular ultrasound (IVUS) is regarded by many physicians as the gold standard in atherosclerosis diagnosis. IVUS is a catheter-based imaging modality which provides real-time and high-resolution tomography visualization of the coronary arteries. Applying the informative rich IVUS frames of each patient and performing manual analysis of cross section area (CSA) images is not only time consuming but also prone to the inter-and intra-observer variability. Hence, developing a device capable of characterizing plaque components by IVUS images automatically is of great importance. The current in-vivo standard for such plaque assessment in IVUS images is the Virtual Histology (VH).[3] VH provides a colored coded plaque characterization image by analyzing the radiofrequency (RF) components of the backscattered ultrasound signal.

However, one of the major VH limitations is the electro-cardiogram (ECG) gated computation. Indeed, owing to RF attenuation and shifting due to presence of blood in coronary arteries, such signal processing approach have to use an ECG gating procedure. Most ECG gating methods provides only one image per cardiac cycle, and this, at the end-diastolic point (peak R-wave). Assessing the plaque histology on only one frame per cardiac cycle significantly decreases the longitudinal resolution of IVUS imaging. Considering a heart rate of 60 bpm and

Further author information: (Send correspondence to Arash Taki)
E-mail: taki@cs.tum.edu, Telephone: +49 177 1344851

Medical Imaging 2010: Ultrasonic Imaging, Tomography, and Therapy, edited by Jan D'hooge, Stephen A. McAleavey,
Proc. of SPIE Vol. 7629, 76290Y · © 2010 SPIE · CCC code: 1605-7422/10/$18 · doi: 10.1117/12.843791

a pullback speed of 1 mm/s, VH can be computed once every 1mm while grayscale IVUS, with an acquisition frequency of 30 frames/s, every $\frac{1}{30}$mm. This means that more than 96 % of acquired information is not accessible with VH and thus, atherosclerotic lesions can not be precisely investigated. Moreover, in some occasional cases, the longitudinal catheter motion of more than 5mm/s has been reported.[4]

Instead of using the backscattered RF signals, image-based techniques would permit to use IVUS images from the whole cardiac cycle, which would definitely increase the longitudinal resolution of such a histology assessment. For this purpose, several feature extraction techniques have been applied and compared in[5] to characterize each pixel of an IVUS frame and to assign it to a tissue class. According to Vince et al,[5] the co-occurrence method showed the best accuracy. In,[6] both signal and image based features are extracted. 90% accuracy is achieved in comparison with manually characterized images by two experts, which would extremely increase the uncertainty of their results, using the co-occurrence, Local Binary Pattern (LBP) , and Gabor filtering methods for feature extraction from the IVUS images. In this paper, we introduce a novel technique to provide a color-coded characterization of the atherosclerotic plaque directly from grayscale IVUS images without the need of RF signals. We propose to characterize each pixel in the plaque area of a grayscale IVUS image by extracting textural information from the relevant sub-bands of the frequency spectrum. Our approach is described as follows:

1. IVUS frame is transformed into polar coordinates to ensure rotation invariance
2. decomposition into a set of multiple sub-band images by using redundant wavelet packet transform
3. run-length matrices are computed from each sub-band image to encode their textural information
4. textural features characterizing each pixel are then extracted from these matrices
5. Relevant sub-bands are selected by using Local Discriminant Bases with Fisher's criterion
6. pixels are assigned to one of the three tissue classes (i.e. DC, NC, and Fibro-Fatty(FF)) by an architecture of weighted support vector machines associated to each selected sub-bands

This method can be performed on all the IVUS frames of the heart cycle and thus permits to outperform the longitudinal resolution of VH. It also gives the possibility of extracting histological information from the large archive of the IVUS images obtained in the past for which RF signals are not available.

The remaining of this paper is organized as follows: Section 2 describes the methods and the proposed algorithm employed to characterize plaque compositions in the plaque area of IVUS images. Section 3 provides comparative results with those obtained from co-occurrence and LBP feature extraction techniques. Since in vivo VH images have been considered as gold standard for plaque assessment, they are used for validating these three techniques. Finally section 4 concludes the paper.

2. METHODOLOGY

IVUS images are circular cross section of the blood vessel. To ensure rotation invariance for the feature extraction, input images are converted into polar coordinates. In the remaining of the paper, I refers to the IVUS image in polar coordinate. Fig. 2 shows the steps of our proposed algorithm for IVUS plaque characterization.
Note that this paper is not proposing a method for detection and extraction of the plaque area. Border detection and extraction of the plaque area within IVUS images which is necessary for such segmentation have been subjects of many research work.[7] *In this paper, we use the plaque area taken directly from the VH characterized images, in order for us to be able to validate the classification method proposed here.*

2.1 Redundant Wavelet Packet Transform

Since each tissue shows different echogenic characteristics, the different plaque components can be characterized by their local frequency components. The Wavelet transform (WT) provides the best approximation of a space-frequency representation of an image, i.e. it permits to know which spectral components exist at which position in our input image I. The main drawback of the WT is its translation non-invariance due to the decimation applied to the image after each decomposition level. Recently, another type of wavelet transforms known as Redundant

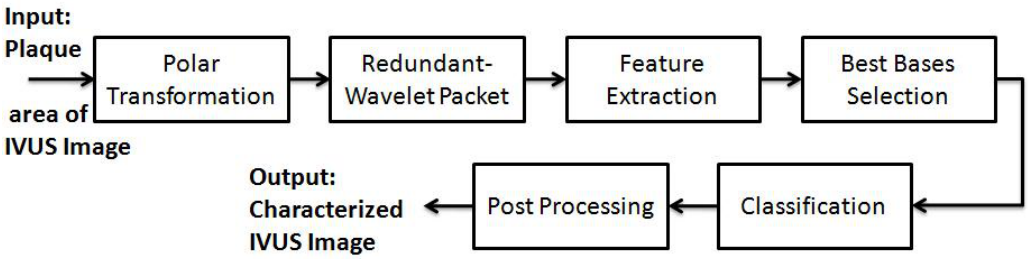

Figure 1. Block Diagram(In this paper, the plaque area is taken directly from the VH examples enabling quantitative validation, see text.)

Wavelet Transforms (RWT) has been introduced.[8] In contrary to the classical WT, there is no decimation step after filtering the input image. This provides translation invariance and, since it preserves the size of images in each level of decomposition, the local spectral components can be retrieved without any interpolation step. To generalize such transform, the Wavelet Packet transform (WPT)[9] has been introduced to decompose the whole frequency spectrum into multiple sub-bands of varying sizes as shown in Fig.2. It has been shown to provide a more redundant representation for the analysis of complex textural information. By combining the RWT and WPT, I can be decomposed into multiple sub-band images while providing translation invariance in addition to the rotation invariance gained by the initial polar transform.

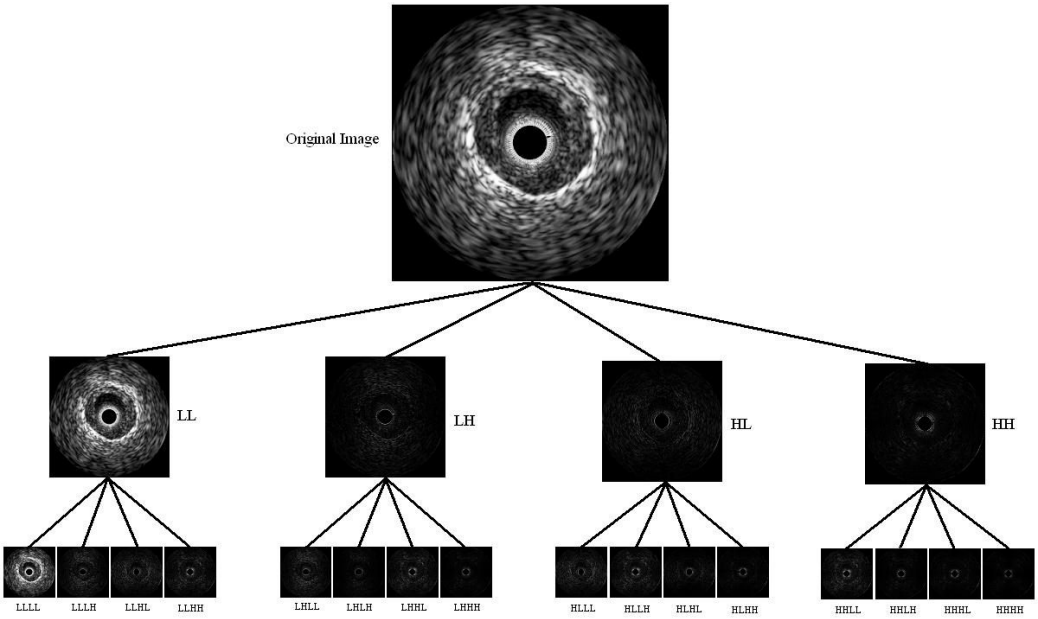

Figure 2. Two level decomposition of RWT+WPT for an IVUS image

2.2 Textural Feature Extraction

Let $\{I_k\}_{k\in\{1,N\}}$ be a collection a N sub-band images extracted from I through redundant wavelet packet transform (RWPT). In this section, we present how to characterize each pixel (x, y) from I with textural descriptors extracted from the $\{I_k\}$. This provides an enhanced extraction of texture information by analyzing the different sub-band of the frequency spectrum. In this paper, our approach based on run-length features is compared to Co-occurrence, and Local Binary pattern (LBP) methods.

Run-length based textural descriptors:
Since most of the discriminative information lies in the homogeneity of specific intensities in different plaque types, we propose an approach based on run-length features. Run-length transform has been extensively used to encode textural information for texture analysis purposes. Let us consider the $V \times W$ neighborhood $\{I_k(i+m, j+n)\}_{m,n}$ with $m \in \left[-\frac{V}{2}, +\frac{V}{2}\right]$ and $n \in \left[-\frac{W}{2}, +\frac{W}{2}\right]$, centered on the pixel (i, j) from the sub-band image I_k. Its run-length matrix is defined in a given direction as $R_k(a, b)$ where $a \in [1, M]$ is the gray level, M is the highest gray level, and b is the run-length, i.e. the number of consecutive pixels along a direction having the same gray level value. In our approach we characterize each neighborhood with two run-length matrices $R_k^x(a, b)$ and $R_k^y(a, b)$ corresponding respectively to x and y directions.

From these run-length matrices, a wide collection of textural features can be derived. To characterize the run-length statistics of such matrices, five features have been introduced by Galloway:[10] Short Run Emphasis (SRE), Long Run Emphasis (LRE), Gray-level Nonuniformity (GLN), Run Length Nonuniformity (RLN), and Run Percentage (RP). Unfortunately, according to,[5] these were not fullfilling to characterize IVUS images. For this reason, we propose the use in addition six run-length-based features introduced later by:[11] Low Gray-Level Run Emphasis(LGRE), High Gray-Level Run Emphasis(HGRE), Short Run Low Gray-Level Run Emphasis(SRLGE), Short Run High Gray-Level Run Emphasis(SRHGE), Long Run Low Gray-Level Run Emphasis(LRLGE) and Long Run High Gray-Level Run Emphasis (LRHGE).

Let us denote $f_k^{\theta,\lambda}(i, j), where \theta = \{x, y\}\ and \lambda = \{1, 2, ..., 11\}$ the 22 features extracted from the neighborhood $\{I_k(i+m, j+n)\}_{m,n}$. Each pixel (i, j) of each image I_k is then characterized by the following set of features $V_{i,j}^k$:

$$V_{i,j}^k = \left\{ f_k^{\theta,\lambda}(i, j) \right\}_{\theta,\lambda} \tag{1}$$

2.3 Best Basis Selection

Principal objective in a classification problem is to extract features that are capable of discriminating different classes as much as possible. Generating a proper feature space highly influences the accuracy of the classification results. The best subset of the $\left\{V^k\right\}_{k\in\{1,N\}}$ has to be chosen out to provide an optimal discrimination power. To this end, we introduce an adapted discriminant measure.

Discriminant Measure:
Discriminant measures have been introduced to evaluate the statistical distance among different classes.[9] In this paper, we propose to use the Fisher criterion for discriminating our 3 tissue classes:

$$D(k, \theta, \lambda) = \frac{(\mu_p^{k,\theta,\lambda} - \mu_q^{k,\theta,\lambda})^2}{{\sigma_p^{k,\theta,\lambda}}^2 + {\sigma_q^{k,\theta,\lambda}}^2} \tag{2}$$

where $\mu_p^{k,\theta,\lambda}$ and ${\sigma_p^{k,\theta,\lambda}}^2$ are respectively the mean and the variance of the component $f_k^{\theta,\lambda}$ of V^k in the p^{th} class. This measure takes high values when the feature is varied in classes such that it has maximum differences in the mean and minimum variances.

Algorithm for Selecting the Best Basis:
After computing the Fisher criterion for each component of all the $\left\{V^k\right\}_{k\in\{1,N\}}$, sub-band which have higher values offer the best discrimination power. We propose to use a variant of the Local Discriminant Basis (LDB) algorithm introduced by Saito and Coifman[9] with Fisher's criterion. This algorithm selects the best subset of the $\left\{V^k\right\}_{k\in\{1,N\}}$ by computing its discrimination power as follows:

$$D(k) = \sum_{\theta} \sum_{\lambda} D(k, \theta, \lambda) \tag{3}$$

Each pixel (i, j) of I is then characterized by the subset of features we denote $\left\{V_{i,j}^k\right\}_{k\in M}$ with $M \subset \{1, N\}$.

2.4 Weighted classification structure based on SVM

For classification, we propose to use a structure of multi-class support vector machines. To each selected sub-band k with $k \in M$, a SVM is associated. However, all sub-bands do not have the same discrimination ability. Therefore, a weight is assigned to each classifier based on its discrimination ability. The final decision for a pixel is attained by considering the weighted votes of all SVMs. To handle non-linear relations between feature vectors and their tissue classes, a gaussian kernel is used to map the input feature vectors to a higher dimension space.

2.5 Post-processing

Studying the intensity distribution of each plaque type in our dataset provides prior information to increase the classification accuracy with a post-processing step. This permits us to define some thresholds to reduce misclassification errors. Indeed, the majority of pixels of the plaque in a typical IVUS image belong to the FF class. However, very few FF pixel intensities exceed the gray-level 150 (considering an intensity range from 0 to 255). Thus, we define a first threshold we denote $ThFF = 150$. If a pixel labeled to FF with an intensity greater than $ThFF$, then it will be classified into one of the two other classes. Since most of pixels with intensities above the gray-level 200 belong to the DC class, we can define the next threshold $ThDC = 200$ to decide between NC and DC classes.

3. RESULTS

The study group used for our experiments consists of sequences of IVUS images acquired from five patients. Out of the frames in which all types of plaques were detected by the VH method, 40 frames were selected for each patient. The three mentioned feature extraction methods were then applied on the set of 200 frames. The characterized IVUS images were validated by their corresponding VH images and the accuracy, sensitivity, and specificity parameters were calculated for each technique.

Since the most important plaque components are fibro-fatty tissues, necrotic core and dense calcified for atherosclerosis staging, we focussed on the classification into these three classes.

The Daubechies 4 wavelet, which has the ability of following small variations, is used for the RWPT decomposition. The number of decomposition levels was set to two, giving thereby 21 sub-band images. The size of neighborhoods, on which features were extracted, was empirically chosen to be 9*9 for all methods. For LBP method, four circles were then constructed in each neighborhood. Then, three features were extracted from each circle.

After computing Fisher criterion for feature vectors of every sub-band images, a subset of 12 were selected based on their discrimination power and LDB procedure. Then, a weight was assigned to each based on their Fisher measure. The computed weights show that subband two (low-frequency) has the best discrimination power in comparison with the others. We used the LIBSVM C++ implementation of the SVM algorithms.[12] A grid-search was performed for optimal parameter selection and a 5-fold cross validation to evaluate the performance of all three methods.

For a typical frame the Run-length method took approximately 2 minutes to extract the features, whereas the LBP needed 20 minutes and the co-occurrence nearly 120 minutes. In terms of time efficiency, the Run-length method further outperform the other two. A MATLAB implementation on an Intel Core 2 CPU 2.00 GHz computer with 2.0 GB Ram was used in this work.

Table 1 illustrates the results using different methods besides the influence of our post processing step. It can be inferred from the results that the run-length feature extraction method has a better capability for classifying DC plaques, while LBP and co-occurrence for NC. Results also show the influence of the post-processing step on the Sensitivity of the NC class. Therefore, one might use the textural features and the classification procedure for dividing the plaque area into two classes, i.e. DC and FF, and then use prior information on their intensity distributions to distinguish the NC regions from them. Still, the sensitivity of all methods for the detection of the NC was low (46%). This fact was caused by similarities between NC and DC in Gray level IVUS images.[13]

Fig. 3 illustrates the images characterized by all methods with their corresponding IVUS and VH images.

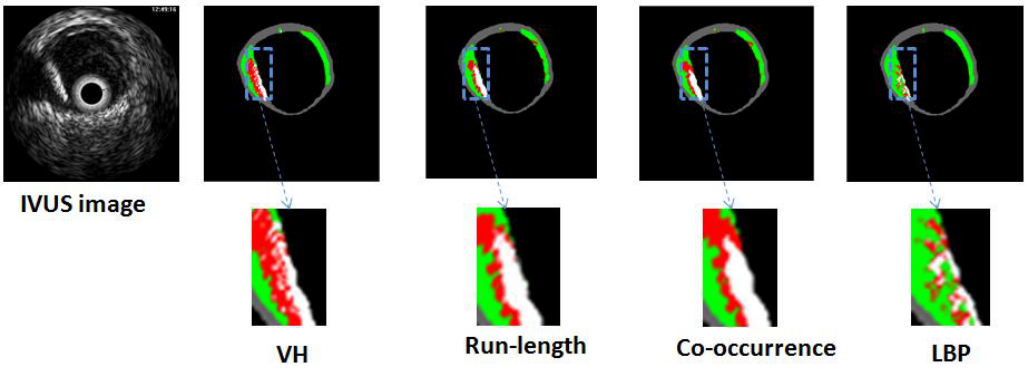

Figure 3. The result of feature extraction methods (White is calcium, Green is fibro-fatty, and Red is Necrotic)

Table 1. Accuracy of the different techniques. Numbers within parenthesis and wihtout relate respectively to before and after post-processing.

Technique	**Overall Accuracy**		**DC**	**FF**	**NC**
Run Length	(73%)72 %	Sensitivity(%)	(76)73	(97)85	(9)42
		Specificity(%)	(93)93	(57)79	(96)84
Co-Occurence	(71%)71%	Sensitivity(%)	(72)70	(97)84	(14)46
		Specificity(%)	(96)96	(58)80	(94)82
LBP	(66%)70%	Sensitivity(%)	(40)59	(97)85	(8)47
		Specificity(%)	(95)95	(37)78	(96)80

4. CONCLUSION

In this paper, we proposed to improve the longitudinal resolution of IVUS-VH. To this end, we introduce an image-based approach to classify each pixel of atherosclerosis plaque into three tissue classes, namely fibro-fatty, necrotic core and dense calcified tissues. The original IVUS frame is converted into polar coordinate and decomposed into sub-band images with a RWPT. Run-length based features are then extracted from the neighborhoods of each resulting image. A combination of LDB and Fisher criterion permits the selection of the sub-bands providing the best discrimination power according to these features.

Results showed the effectiveness of the Run-length features in comparison to the co-occurrence and the LBP methods in terms of both time efficiency and classification accuracy. They also highlighted the benefit of using prior information based on the intensity distribution of each plaque component as a post-processing step.

We evaluated our image-based technique against VH, which is a signal processing approach. Since both of these techniques have their pitfalls, it would be of a great interest to validate the proposed method against a ground truth obtained by histology. As mentioned earlier, the number of classes was reduced to three classes instead of four, by combining the fibrous and fibro-lipid classes. The next challenge is to further discriminate these plaque components.

REFERENCES

1. E. J. Topol, *Textbook of Cardiovascular Medicine*, Lippincott Williams & Wilkins, 3 ed., 2007.
2. R. Virmani, F. D. Kolodgie, A. P. Burke, A. Farb, and S. M. Schwartz, "Lessons from sudden coronary death a comprehensive morphological classification scheme for atherosclerotic lesions," *Arterioscler Thromb Vasc Biol.* **20**, pp. 1262–1275, 2000.
3. A. Nair, M. P. Margolis, B. D. Kuban, and D. G. Vince, "Automated coronoary plaque characterisation with ivus backscatter_ex vivo validation," *EuroIntervention.* , 2007.
4. S. de Winter, R. Hamers, and et al., "A novel retrospective gating method for intracoronary ultrasound images based on image properties," *Computers in Cardiology* **30**, pp. 13–16, 2003.
5. D. Vince, K. Dixon, R. Cothren, and J. Cornhill, "Comparison of texture analysis methods for the characterization of coronary plaques in intravascular ultrasound images," *Computerized Medical Imaging and Graphics* **24**, pp. 221–229, 2000.
6. S. Escalera, O. Pujol, J. Mauri, and P. Radeva, "Intravascular ultrasound tissue characterization with sub-class error-correcting output codes," *Journal of Signal Processing System* , 2008.
7. G. Unal, S. Bucher, S. Carlier, and et al, "Shape-driven segmentation of the arterial wall in intravascular ultrasound images," *IEEE Transactions on Information Technology in Biomedicine* **12**(3), pp. 335–347, 2008.
8. G. P. Nason and B. W. Silverman, "The stationary wavelet transform and some statistical applications," *Nason95thestationary, Springer-Verlag* , pp. 281–300, 1995.
9. R. R. Coifman and M. V. Wickerhauser, "Entropy-based algorithm for best basis selection," *IEEE Transactions on Information Theory* **38**(2), pp. 713–718.
10. M. M. Galloway, "Texture analysis using gray level run lengths," *Comput. Graphics Image Process.* .
11. X. Tang, "Texture information in run length matrices," *IEEE Transactions on Image Processing* **7**(11), pp. 1602–1609.
12. C. Chang and C. Lin, "Libsvm: a library for support vector machines," *Software available at http://www.csie.ntu.edu.tw/ cjlin/libsvm* .
13. F. Sales, J. Falcao, B. Falcao, and et al, "Evidences of possible necrotic-core artifact around dense calcium in virtual histology images,," *Computers in Cardiology Conference* , pp. 545–548, 2008.